Journal of Microscopy

Journal of Microscopy, Vol. 00, Issue 0 2017, pp. 1–19 doi: 10.1111/jmi.12639
Received 3 March 2017; accepted 21 August 2017

Potential of CLSM in studying some modern and fossil palynological objects

O. GAVRILOVA*, N. ZAVIALOVA†, M. TEKLEVA† & E. KARASEV†,‡
*Russian Academy of Sciences, V.L. Komarov Botanical Institute, St. Petersburg, Russia
†Russian Academy of Sciences, A.A. Borissiak Paleontological Institute, Moscow, Russia
‡Kazan Federal University, Kazan, Russia

Key words. Confocal laser scanning microscopy (CLSM), light microscopy (LM), megaspores, pollen grains, scanning electron microscopy (SEM), transmission electron microscopy (TEM).

Summary

We have tested possibilities and limitations of confocal laser scanning microscopy to study the morphology of pollen and spores and inner structure of sporoderms. As test objects, we used pollen grains of the modern angiosperm *Ribes niveum* (Grossulariaceae) and *Datura metel* (Solanaceae), fossil angiosperm pollen grains of *Pseudointegricorpus clarireticulatum* and *Wodehouseia spinata* dated to the Late Cretaceous, fossil gymnosperm pollen grains of *Cycadopites*-type dated to the Middle Jurassic, and fossil megaspores *Maexisporites rugulaeferus*, *M. grosstriletus*, and *Trileites* sp. dated to the Early Triassic. For comparative purpose, we studied the same objects with application of conventional light, scanning electron (to entire pollen grains and spores or to semithin sections of their walls), or transmission electron microscopy. The resolution of confocal microscope is much lower than that of electron microscopes, as are its abilities to reconstruct the surface patterns and inner structure. On the other hand, it can provide information that is unreachable by other microscopical methods. Thus, the structure of endoapertures in angiosperm pollen grains can be directly observed. It is also helpful in studies of asymmetrical pollen and pollen grains bearing various appendages and having complicated exine structure, because rotation of 3-D reconstructions allows one to examine all sides and structures of the pollen grain. The exact location of all visible and concealed structures in the sporoderm can be detected; this information helps to describe the morphology and inner structure of pollen grains and to choose necessary directions of further ultrathin sectioning for a transmission electron microscopical study. In studies of fossil pollen grains that are preserved in clumps and stuck to cuticles, confocal microscope is useful in determining the number of apertures in individual pollen grains. This can be done by means of virtual sections through 3-D reconstructions of pollen grains. Fossil megaspores are too large and too thick-walled objects for a confocal study; however, confocal microscope was able to reveal a degree of compression of fossil megaspores, the presence of a cavity between the outer and inner sporoderm layers, and to get some information about sporoderm inner structure.

Correspondence to: O. Gavrilova, Russian Academy of Sciences, V.L. Komarov Botanical Institute, ul. Professora Popova 2, St. Petersburg 197376, Russia. Tel: +7911-918-4581; fax: +7(812)-372-54-43; e-mail: olgaangav@gmail.com

Introduction

Detailed morphological descriptions of pollen and spores serve as a basis for various palynological studies; and the morphology and ultrastructure of pollen and spores are widely used for systematics and phylogeny of different plant groups as well as for pollen analysis, stratigraphy, melissopalynology, aeropalynology etc. Palynological data are especially important for palaeobotany, where pollen and spores are often the only available well-recognised remains owing to the small size and resistant sporopollenin walls. Apart from dispersed pollen grains and spores, those preserved in anthers, sporangia and micropyles of seeds are very valuable, although occur much more rarely. Such finds provide information about parent plants that produced a given type of pollen or spores. Associations of pollen grains and seeds not only inform about the botanical affinity of the pollen grains, but also allow the scientists to reassembly female and male reproductive organs preserved as detached fossils but contained the same pollen type and, therefore, contribute to whole-plant reconstructions. Morphological information obtained from fossil pollen and spores (in spite of the fact that overwhelming majority of them are strongly flattened) is comparable with that from pollen and spores of modern plants. This makes the inclusion of palynological information on fossil and extant members of higher plant taxa in phylogenetic analysis possible.

Most often, pollen and spores are from 20 to 50 μm in size, rarely 5–10 μm, sometimes up to 130 μm, whereas

megaspores are ranging from 200 to 1000 μm in diameter (occasionally, larger). Thus, even for studying the general architecture of such objects a microscope is needed. First of all, a light microscope (LM) is used but its capability to reveal the inner structure of sporoderms is limited. The pollen wall thickness varies from 0.3 to 0.5 μm to 10 μm or up to or more than 20 μm together with supratectal elements (as in Malvaceae pollen; Christensen, 1986), whereas megaspore walls can reach several dozens of micrometres. The fine sculpture and sometimes sporoderm ultrastructure (Zavialova & Karasev, 2017) are studied with scanning electron microscopy (SEM); the sporoderm ultrastructure is usually studied with transmission electron microscopy (TEM). Electron microscopy, especially TEM, is a more laborious and expensive method than LM. For example, one needs to transfer fossil palynological objects from LM slides to SEM stubs. Special chemical treatment, embedding into resin, and ultramicrosectioning are necessary for a TEM study. Partial loss of valuable fossil material during such manipulations is almost inevitable; only a part of the object is remained after processing for TEM for further studies. A search for alternative nondestructive or complementary methods has been constantly carrying on. One of such methods allowing a more detailed morphological description of pollen and spores is confocal laser scanning microscopy (CLSM). The same slide as for LM is used but capabilities of CLSM are much higher and often unique in comparison to LM. The outer sporopollenin wall has a natural fluorescence so no staining by fluorophores is needed for CLSM.

Modern pollen grains were studied with CLSM by Salih *et al.* (1997), Liu *et al.* (2009), Castro *et al.* (2010), Wang *et al.* (2011), Gavrilova (2012, 2014a,b), Sivaguru *et al.* (2012, 2016) and Mander & Punyacena (2014). Different tasks were set by these authors such as comparisons of the texture and sculpture of Poaceae pollen (Salih *et al.*, 1997), pollen descriptions in CLSM of different taxa (Castro *et al.*, 2010; Gavrilova, 2012, 2014b; Sivaguru *et al.*, 2012), estimation of the volume and density of pollen grains (Golovko *et al.*, 2011), determination of apertural regions in developing tetrads (Banks *et al.*, 2006) and a study of microsporogenesis (Wang et *al.*, 2011). In some studies, pollen grains were prestained by basic fuchsin (Banks *et al.*, 2006), acridine orange (Liu *et al.*, 2009; Wang *et al.*, 2011) and Phloxine B or Periodic AcidSchiff (Sivaguru *et al.*, 2016). Liu *et al.* (2009) and Gavrilova (2012, 2014a) indicated that CLSM provides more information on the pollen and exine structure by studying optical sections of objects and making reconstructions of whole objects. Sivaguru *et al.* (2012) made a comparison of different methods in their study of three different pollen types: widefield, apotome, confocal and two-photon microscopy by reflected light techniques, and bright field and differential interference contrast microscopy (DIC) by transmitted light techniques. Sivaguru *et al.* (2016) used CLSM for a comparison with airyscan and structured illumination superresolution microscopy in a study of several modern and fossil pollen types. Hochuli & Feist-Burkhardt (2004, 2013), Zhuo *et al.* (2006), Peyrot *et al.* (2007), Zavialova *et al.* (2014a,b), Mander & Punyacena (2014), Tekleva *et al.* (2015), Schopf *et al.* (2016) and Zavialova *et al.* (2017) applied CLSM for morphological descriptions of fossil pollen and/or spores, and Shute *et al.* (1996) for cryptospores. Scott & Hemsley (1991) compared laser scanning microscopy (LSM), scanning acoustic microscopy (SAM), SEM and TEM of the fossil spore ultrastructure and concluded that LSM can be successfully applied for this purpose. Although Hemsley (1990), Scott & Hemsley (1991, 1993) observed semithin sections of megaspore walls in LSM, we tried to apply CLSM for megaspores without their destruction and to make a 3D image of their inner structure (Gavrilova *et al.*, 2015). Morbelli (1995), Morbelli & Rowley (1996) studied the wall inner structure of modern *Selaginella* megaspores in CLSM with different fluorochromes. A comparison of these data with those in TEM showed that the same structures can be detected in virtual and/or optical sections of CLSM and ultrathin sections in TEM.

Judging from the above works, we decided that CLSM can be helpful and quite easily used for various palynological objects without additional treatment. The paper is aimed to evaluate the application of CLSM to palynological objects, including those from geological deposits of different ages. It is well understood that CLSM cannot overcome EMs by resolution. We were more interested to profit from advantages of CLSM than to confirm once more the shortages. We have tried to select materials which would allowed to use the best sides of CLSM, to extract information that was unreachable with help of other types of microscopes or that was more difficult to obtain by other microscopes. We have observed several types of modern and fossil pollen and spores with help of CLSM and compared obtained data with the results obtained for the same objects by means of light and/or electron microscopy. Our objects were modern and fossil angiosperms pollen grains, fossil gymnosperm pollen grains, and megaspores of fossil lycopsids.

Angiosperm pollen grains are usually quite small to hope that CLSM will show itself to advantage. What it is able to do (by comparison with EMs) is to observe an intact object from the inside. Another promising quality of CLSM is its ability to turn the reconstruction of the object and observe it from different sides. Angiosperm pollen grains are extremely diverse in morphology. Among them, we have chosen a few morphological types that have complicated numerous apertures, various appendages, and asymmetrical morphology. In addition, the chosen morphological types of angiosperm pollen grains are important for stratigraphy and/or plant phylogeny.

A weaker hope that we nonetheless were determined to test was the ability of CLSM to reconstruct the surface details. We also hoped that a CLSM reconstruction of the surface pattern could have substituted SEM observations of few pollen grains that were discovered in the micropyle of a fossil gymnospermous seed. These pollen grains represent a very rare and

important record of pollen grains found in a seed that supposedly belongs to ginkgoaleans. Male sporangia of ginkgoaleans are usually preserved as opened sporangia without pollen grains or with solitary pollen grains, which amount is insufficient for a solid morphological study. Because of this reason, no data on the fine morphology have been so far available about pollen grains from sporangia of fossil ginkgoaleans. Our study of ginkgoalean pollen grains found in seeds (Zavialova *et al.*, 2014a,b) is the only report about the inner structure of pollen grains of fossil ginkgoaleans. On the one hand, the material at hand was very valuable; on the other hand, the few pollen grains, inseparable from the cuticle, were not very suitable for a destructive electron-microscopical study. Our few pollen grains could have been easily lost during preparation for SEM and processing after SEM. The nondestructive nature of confocal microscopy was very important for the unique material. We also tried to differentiate digitally with help of CLSM between the cuticle and pollen grains that stuck to it, which could have been very helpful for similar fossil materials.

Successful studies of megaspores of modern lycopsids (Morbelli & Rowley, 1996) inspired us to test CLSM on fossil lycopsid megaspores.

Material and methods

Pollen grains of modern *Ribes niveum* Lindl. (Grossulariaceae) were gathered from two bushes, the first grows in the garden of Komarov Botanical Institute of the Russian Academy of Sciences, St. Petersburg, Russia (BIN) and the second is from the collection of black currant and gooseberry NPB 'Pushkin and Pavlovsk laboratory VIR', St. Petersburg, Russia. Pollen grains of modern *Datura metel* L. (Solanaceae) were collected in the greenhouse of Komarov Botanical Institute of the Russian Academy of Sciences, St. Petersburg, Russia (BIN). The pollen grains were acetolysed after Erdtman (1952) and observed with LM, CLSM, SEM and TEM in BIN. Pollen grains of *R. niveum* and *D. metel* have been studied with a Micmed-6 (LOMO, St. Petersburg, Russia) LM in palynological laboratory of BIN and with a JEOL JSM-6390 (Jeol Ltd., Peabody, Massachusetts, USA) SEM and a Hitachi-H600 (Hitachi, Ltd., Tokyo, Japan) TEM at the Core Centrum 'Cell and Molecular Technologies in Plant Science' in BIN. For TEM, flower buds of *R. niveum* have been fixed with 2.5% glutaraldehyde in 0.1 M phosphate buffer pH 7.2 and stained with 1% OsO_4 and 0.5% uranyl acetate. The material was dehydrated in alcohols and acetone series and enclosed in epon by a standard method. The sections were additionally poststained with uranyl acetate and lead citrate.

Fossil pollen grains of *Pseudointegricorpus clarireticulatum* (Samoilovitch) Takahashi (Tekleva *et al.*, 2015) and *Wodehouseia spinata* Stanley came from the Upper Maastrichtian, in Zeya-Bureya Basin, Amur (Heilongjiang) River area, Russian Far East (Markevich *et al.*, 2011). The pollen treatment and used facilities are described in Tekleva *et al.* (2015).

Pollen grains of *Cycadopites*-type were found in the pollen chamber of a dispersed seed of *Allicospermum angrenicum* Nosova from the Middle Jurassic locality of Angren in Uzbekistan; pollen treatment, methods and equipments are after Zavialova *et al.* (2014a).

Dispersed megaspores of *Maexisporites rugulaeferus* Karasev et Turnau 2015, *M. grosstriletus* (Liu *et al.*, 2011) Karasev et Turnau, 2015 and *Trileites* sp. were collected from the Sholga locality, lowermost Triassic sediments of the Moscow Syneclise in Russia. Collection PIN #5529 (Sholga locality) is kept at the A.A. Borissiak Paleontological Institute, Russian Academy of Sciences, Moscow, Russia (PIN). The megaspores were isolated from the encompassing sediments by disintegration in water followed by treatment with HCL, again water and finally by HF for cleaning from silica component. The megaspores were picked from a Petri dish with a needle and mounted on SEM stubs to study their general morphology. It was accomplished under a TESCAN VEGA-II XMU (Tescan, Brno, Czech Republic) SEM (accelerating voltage 30 kV) at PIN.

For a comparison with CLSM data, the inner structure of megaspores was observed in ultrathin sections in TEM or semithin sections in SEM. For TEM, the megaspores were embedded in a mixture of epoxy for 48 h at 62 °C. Sectioning was accomplished with a Leica EM UC6 (Leica Microsystems GmbH, Wetzlar, Germany) ultramicrotome at PIN. Sections of 70 nm were observed unstained under a Jeol 100B (Jeol Ltd., Peabody, Massachusetts, USA) TEM (accelerating voltage 80 kV) at the Electron Microscope Laboratory of the Lomonosov Moscow State University (MSU). Semithin sections of 1 μm thick were made either from PVP-sucrose blocks (after Chentsov *et al.*, 1973) or from the same epoxy blocks, which were made for TEM. The epoxy was solved after Maxwell (1978). The epoxy-free sections were mounted on SEM stubs and viewed in SEM (after Zavialova & Karasev, 2017).

For CLSM, all pollen and megaspores have been studied with a Zeiss LSM 780 (Carl Zeiss AG, Oberkochen, Germany) CLSM at the Core Centrum 'Cell and Molecular Technologies in Plant Science' in BIN after Gavrilova (2014b). Unstained pollen or spores were mounted in glycerin and/or glycerin jelly slides. We accomplished spectral scan. Although palynological objects vary in autofluorescence, they vary within the 610–690 nm range, as we discovered on all palynological objects we have ever tested with CLSM. Data by other authors agree with our observations (e.g. Castro *et al.*, 2010). We used a 99 μm pinhole, a 561 emission wavelength, a 561-nm laser (which is more suitable for unstained palynological objects), and mainly a 63 × 10 oil immersion objective. Megaspores have been analysed with a 40 × 10 oil immersion objective; fragments of sporoderms have been scanned with a 100 × 10 ones. To obtain the object reconstruction, we used a distance between optical sections from 0.2 to 0.4 μm. Usually, we used the option Brightness Correction in a deeper focus position. We applied it once or twice to the same z-stack depending on the thickness and/or density of the object. The imaging,

3D reconstructions, and measurements were made using Zen 2011 and Zen 2012 imaging software. To describe morphological details of the objects under study, we took optical sections, reconstructed objects and their parts, and also made arbitrarily directed sections through the reconstructions. We prefer to apply «transparent» or «mixed» 3D visualisation techniques for the evaluation of fine outer and inner structures; maximum intensity projection and «shadow» or «surface» options of image processing have been used for displaying architectural and surface features.

Pollen size measurements were made in LM and CLSM. Exine and surface details were measured in SEM and TEM images and CLSM software. The terminology used follows Punt *et al.* (2007), Hesse *et al.* (2009) and some original descriptions.

Results and discussion

Pollen grains of modern angiosperms

Pollen grains of *Ribes niveum* (Figs. 1A–R) are 4- or 5-zonocolporate with two ora per one colpus. The pollen grains are spheroidal and medium-sized from 22.9 to 32.1 μm in diameter. The outline is rounded or lobate from the polar view and mainly rounded from the equatorial view. The colpi are wide (around 4 μm), with curved tips in the apocolpium; the margins of colpi are indistinct. The ora are rounded from 3.1 to 4.3 μm in diameter, distinct, situated in the colpi closer to the pole. LM shows a thin exine about 1.0–1.8 μm thick, which supposedly includes two layers, and a rough or psilate sculpture.

Dentate margins of colpi, small dense nanoparticles on the mesocolpium and rare particles on the membrane of the colpi are detected by CLSM (Figs. 1I–K). A three-dimensional reconstruction of the pollen and its rotation show that not all grains have regular colpus disposition, sometimes one colpus merges with adjacent colpi in the apocolpium (Fig. 1I). CLSM optical sections demonstrate two layers of the exine and some exine thickenings near ora (Figs. 1N–O). The difference between ectexine and endexine is not visible with help of CLSM.

In SEM, the exine sculpturing is microechinate with small dentate echini about 0.1 μm and an irregularly arranged granulate surface of the colpus membrane with round or angular granules about 0.1–0.3 μm (Fig. 1L).

Only TEM data show the fine structure of the sporoderm. For TEM investigation, we processed nonacetolysed pollen, with the intine in their sporoderm (Figs. 1M, P–R). The exine and intine layers are clearly distinct from each other. Ectexine is about 0.5 μm thick, we observed a thin nonuniform endexine 0.4–0.5 μm thick, which is thicker under the colpus up to 1 μm. The infratectum is granular with granules separated from the tectum; angular granules on the colpus membrane are of the same nature. The tectum is continuous with small echini and occasional microperforations. TEM shows that the pollen grains do possess compound apertures, consisting of ectoapertures and endoapertures.

To conclude, CLSM turned to be very suitable to study asymmetrical pollen. Pollen grains of the Grossulariaceae have various ectoapertures; often, their ectoapertures are disposed irregularly (Gavrilova & Tikhonova, 2013; Gavrilova *et al.*, 2017). These palynological characters have diagnostic and taxonomic significance. A CLSM three-dimensional reconstruction and the possibility of the pollen grain rotation with CLSM helped us to describe correctly all types of irregularities, that is useful for systematics, botany and pollen analysis. In this family, only pollen grains of *R. niveum* have microechinate sculpture, but this feature is clearly distinguishable with SEM, but indistinguishable with LM or CLSM. The sporoderm fine structure is observable in full detail only with TEM.

Pollen grains of *Datura metel* (Figs. 2A–P) are 3-colporate, spheroidal or subspheroidal, medium-sized 35.6–45.9 μm × 32.5–49.8 μm in diameter. The outline is rounded or slightly elliptic in equatorial view, and rounded or rounded triangular in polar view. By LM data, pollen may be defined as cryptoaperturate: colpi are not clear. The endocingulum (a ring-shaped continuous endoaperture around the equator) is visible, with indistinct margins. Some exine thickenings formed by the endocingulum are visible. The exine is tectate, columellate, and about 2.3 μm thick. The sculpture is striate, the striae are long, meridionally oriented and rarely branched.

CLSM (Figs. 2E–L) shows indistinct short colpi, 15.8–25.1 μm long and 3.2–16.0 μm wide. The exine is tectate and columellate. Optical sections demonstrate exine thickenings around endocingulum margins and at the endocingulum/colpus border. The endocingulum is 5.9–11.6 μm wide. The exine is 2.0–2.5 μm thick, becoming up to 5.1 μm in endocingulum margins and up to 6.3 μm around the colpi. The ectexine is indistinguishable from the endexine, and we cannot precisely define whether the thickenings are formed by the ectexine or endexine, but we suppose that the thickenings are endexineous. The exine in the endocingulum is thin (1.8 μm) and is formed only by a tectum and sometimes by an infratectum. The columellae are distinct, 0.3–0.5 μm wide. The sculpture is striate, with perforations about 1 μm in diameter (seen in optical sections through the exine and in pollen grains reconstructed and presented in 'transparent' mode) between the striae. The striae are long, meridionally oriented, 0.8–1.3 μm wide, becoming wider (up to 2.6 μm) near the colpi.

In SEM (Figs. 2M–P), pollen grains seem to be inaperturate. Pollen grains are spheroidal, striate-perforate, the striae are meridionally oriented, 0.8–1.3 wide, with perforations of 0.7–1.2 μm in diameter between the striae and microgranules on the striae. The granules smaller than 0.3 μm in diameter are distinguishable only in SEM.

Previously, pollen grains of this and other species of *Datura* with an endocingulum have been described as 3-colporate (Peng *et al.*, 1985), 3-zonocolporate with indistinct

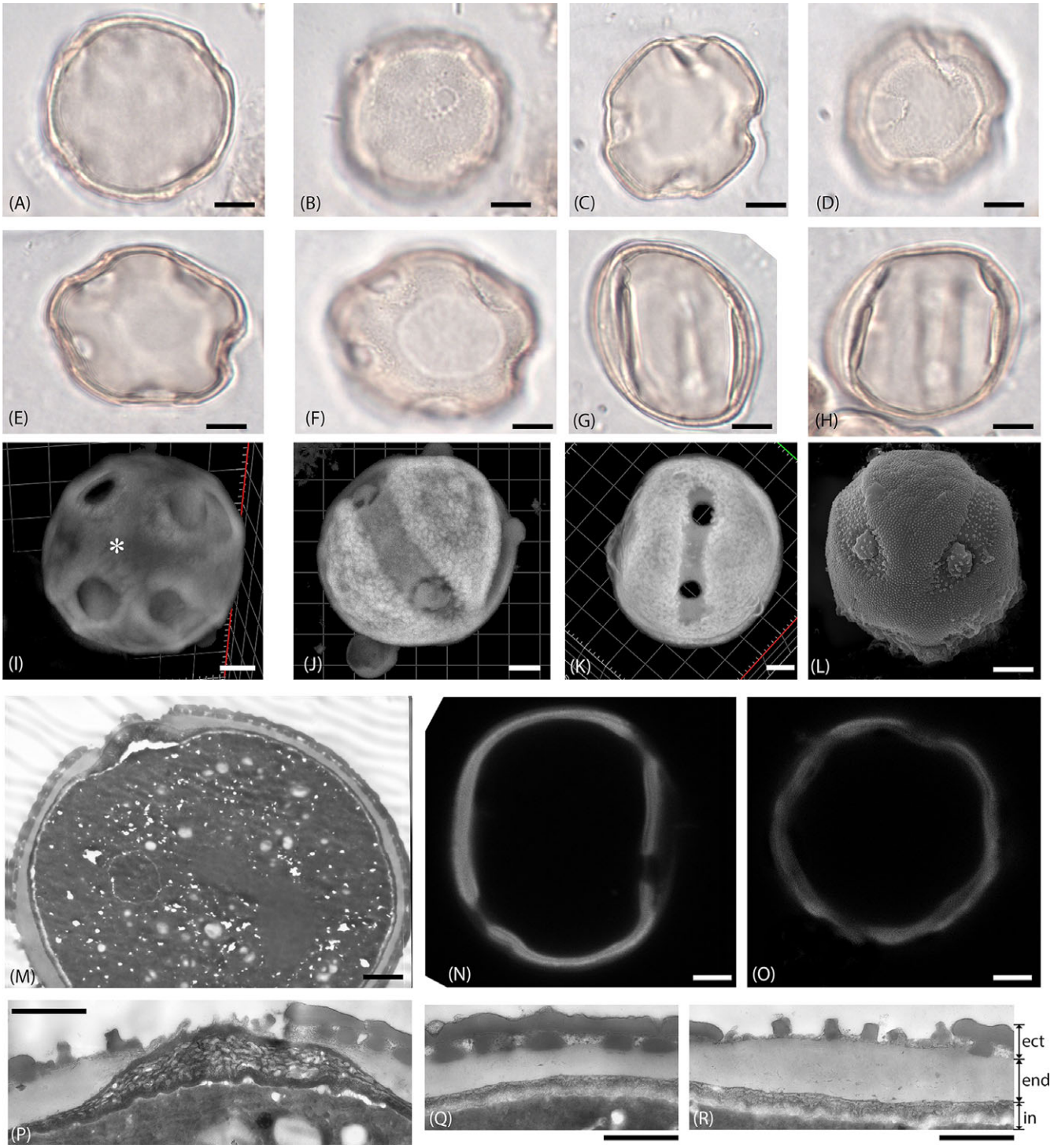

Fig. 1. Pollen grains of *Ribes niveum*. (A–H) LM, (I–K, N, O) CLSM; (L) SEM; (M, P–R) TEM. (A–F, I, L) Polar view; (G, H, J, K) equatorial view; (N, O) optical sections; (I) polar view of reconstructed pollen grain, transparent mode, two left colpi are merged in the pole (asterisks); (J) equatorial view of reconstructed pollen grain, maximum mode; (K) equatorial view of reconstructed pollen grain, transparent mode; (M) section of the main part of a whole pollen grain, intine and exine layers are clearly seen; (P, R) section of sporoderm in apertural region; (Q) section of sporoderm in nonapertural region; (R) intine (in), ectexine (ect) and endexine (end) are indicated. Scale bars: (A–L, N, O) 5 μm; (M) 2 μm; (P, R) 1 μm; (Q) 0.5 μm.

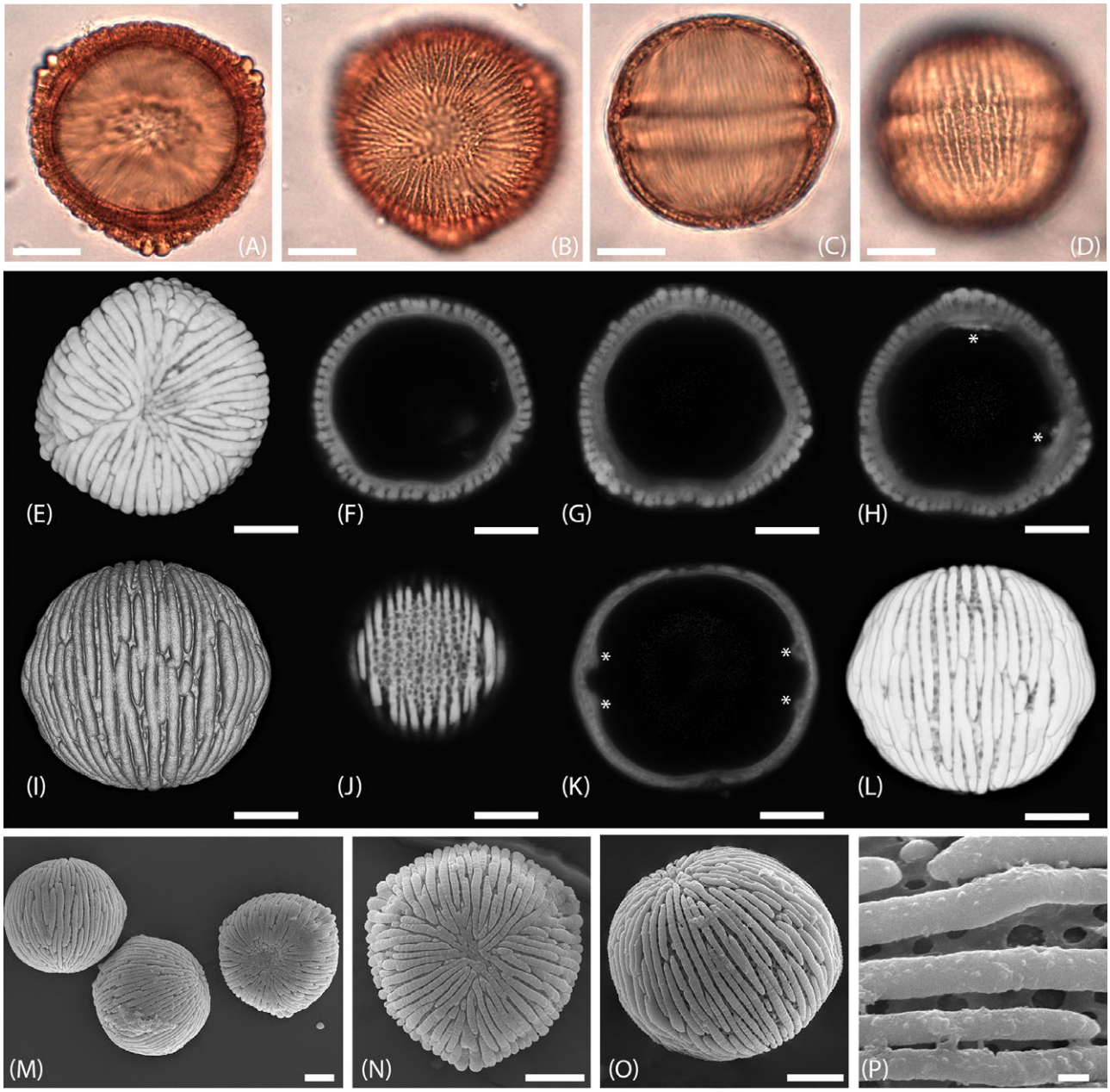

Fig. 2. Pollen grains of *Datura metel*. (A–D) LM; (E–L) CLSM; (M–P) SEM. (A, B, E–H, N) polar view; (C, D, I–L, O) equatorial view; (A, C) focus on the exine structure; apertural margins (A, C) are not well determined; detectable pollen ornamentation is striate (B, C); (F–H, J, K) optical sections; (E) polar view of reconstructed pollen grain, transparent mode; (F–H) optical sections at different depths of the scanning of the grain from pole to pole; (I) equatorial view of reconstructed pollen grain, surface mode; (J, K) optical sections at different depths of the scanning of the pollen grain in equatorial position; (L) equatorial view of reconstructed pollen grain, transparent mode; (P) pollen ornamentation; striate-perforate exine is notable in optical section (J) and in transparent mode of equatorial view (L); granules on the striae are visible only in SEM micrographs (P), exine thickenings and aperture margins (asterisks) are detectable in optical sections (H, K). Scale bars: (A–O) 10 μm; (P) 1 μm.

ectoaperture and endoaperture margins (Persson *et al.*, 1999), 3-colporate, zonoaperturate, with a short ectoaperture (= colpus), which is not sunken, with irregular margins and acute ends, and a circular endoaperture (Perveen & Qaiser, 2007), 3-zonocolporate with indistinct endoaperture margins (Al-Quran, 2004), 3-colporate and 3-colpate (www.paldat.org/search/genus/Datura). Species of *Datura* vary by details of the exine sculpture. In the Solanaceae, an endocingulum has been found in pollen of such closely related to *Datura* genera as *Browallia, Brugmansia, Jaborosa* and

Table 1. The possibilities of use of different microscopes at palynological research.

	LM	CLSM	SEM	TEM
Pollen/spore size	+	+	±	–
Pollen/spore shape	+	Even better	±	–
General sculpture type	Poor	Good	Good	–
Sculpture elements	Usually unavailable	Good when sculpture elements coarser than 0.3 μm	Good	–
Morphological peculiarities (e.g. projections)	Good	Even better	Depend	Depend
Aperture condition	Good	Even better	Depend	Depend
Exine layer stratification (contrast, distinctiveness)	Poor	Some features are discernible	Some features can be observed on broken walls	Good
Ectexine structure	Infratectum type can be sometimes seen	Some features are discernible	Some features can be observed on broken walls	Good
Endexine structure	Usually not distinguishable	Thickness and sometimes structure can be detected	Thickness can be measured at broken walls	Good
Ultrastructural peculiarities (different thickenings, cavities, inner surface of the aperture etc.)	Some can be seen	Most can be seen	Few can be seen	Depend

Streptosolen as well as in a quite distant *Solanum* and some other taxa (Persson *et al.*, 1999; Al-Quran, 2004; Perveen & Qaiser, 2007; our unpubl. data). Pollen grains with an endocingulum occur in other families and sometimes are named as pollen grains with a colpus equatorialis or zonorate pollen. Thus, similar endoapertural structures were reported in pollen of *Polygonum convolvulus* (Polygonaceae http://www.pollen.mtu.edu/glos-gtx/glos-p2.htm), Apiaceae species (elongated endoapertures forming an endocingulum http://www.geo.arizona.edu/palynology/pid00043.html), *Centaurea alpina* (Asteraceae, Siljak-Yakovlev, 1986), some species of *Tabernaemontana* (Apocynaceae) described as 'an equatorial belt or transversally elongated endoapertures' (Nilsson, 1986), some species of *Lonicera* and *Zabelia* (Caprifoliaceae, our unpubl. data) and in some members of the Sapotaceae (Harley, 1986). Pollen grains with an endocingulum have various exine ornamentation and stratification. This pollen type may be compressed into pollen with three equatorial projections, which are formed by exine thickenings, and it may be similar to fossil pollen grains of Triprojectate group. Our results on pollen grains of modern angiosperms have shown that CLSM is useful for studies of medium-sized pollen grains with a complicated inner structure; 3-D reconstruction of pollen grains and an option to rotate such reconstructions allow one to understand possible transformations of the pollen grains, and additional data obtained by means of CLSM about the pollen morphology can help to elucidate the relationships of the plant. A comparison with EMs has shown relatively limited capabilities of CLMS to reveal fine structural details of the exine.

In sum, in comparison to LM, CLSM has a higher resolving power: CLSM images permit to see the exine stratification, inner surface of the pollen wall and exine sculpture, excluding particles smaller than 0.3 μm (Table 1). The division of exine layers into ectexine and endexine is possible only with TEM: it is shown that the foot layer in pollen grains of *Datura stramonium* (www.paldat.org/search/genus/Datura) is discontinuous and the endexine is compact continuous and quite thick. Published TEM images of the exine of *D. metel* are overcontrasted and no description of the exine was provided (Sangwan & Sangwan-Norreel, 1980). However, the layer underlying the columellae seems to be lamellate. Therefore, there is a possibility that the inner layer is represented by an endexine. If this is the case, our assumptions about the endexineous nature of the thickenings around the endocingulum appear to be correct. Other characteristics of the exine, such as the structure of the tectum and infratectum and the relative thicknesses of the exine layers, are seen with help of CLSM in sufficient detail in comparison with TEM data.

Pollen grains of fossil angiosperms

Dispersed pollen grains of *Pseudointegricorpus clarireticulatum* (Figs. 3A–G), previously studied by Tekleva *et al.* (2015), belong to Triprojectate group. By LM data, pollen grains of *P. clarireticulatum* are medium-sized, about 61 × 37 μm, isopolar to subisopolar, tricolpate, and with three additional equatorial furrows. CLSM allowed us to measure the lengths of all the three equatorial projections (8.5–13.5 μm) and furrows (14–16 μm). By comparison with LM, CLSM optical sections demonstrate the following exine layers: an ectexine of 1.2–1.9 μm thick with a tectum, a collumelate infratectum and foot layer, and an endexine of 0.8 μm thick, with thickenings (up to 3.0 μm) around regions adjacent to

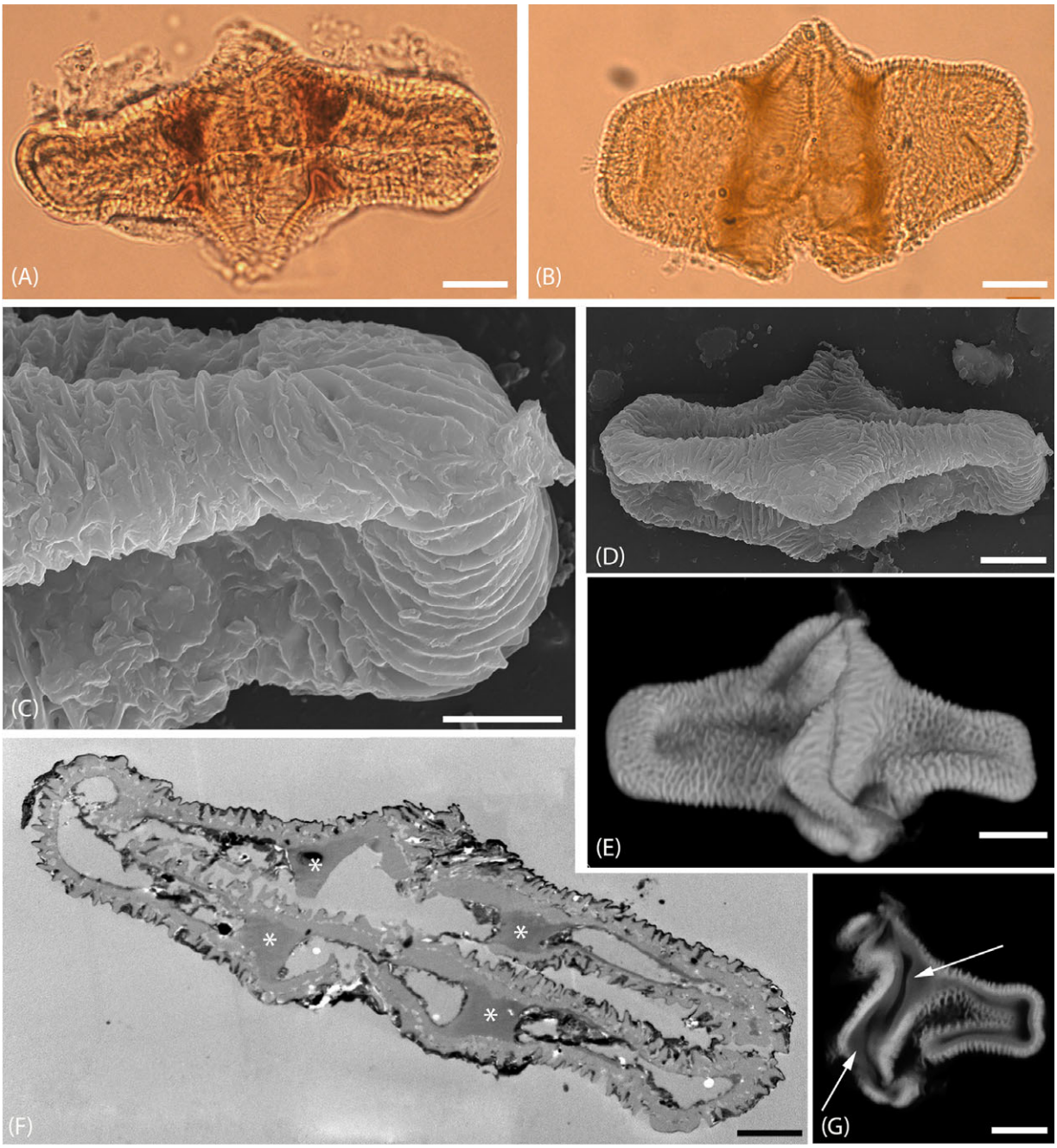

Fig. 3. Pollen grains of *Pseudointegricorpus clarireticulatum*. (A, B) LM; (C, D) SEM; (E) CLSM; reconstructed pollen grain, transparent mode; (F) TEM; (G) CLSM, optical section of a half of a pollen grain. (A) exine thickenings are visible; (B) exine sculpturing and columellate infratectum are seen; (C) polar projection of the pollen, reticulate sculpture is clearly seen; (D, E) an overview of the pollen with two polar and three equatorial projections, colpi and additional equatorial furrows are clearly seen; (F) longitudinal section of a whole pollen, ectexine layers and endexinous thickenings (asterisks) are clearly seen; (G) optical longitudinal section through half of a pollen grain, ectexine as a lighter layer and endexinous thickenings (arrows) can be distinguished. Scale bars: (A, B, D, E, G) 10 μm; (C, F) 5 μm.

the furrows. CLSM provides images of the pollen ornamentation with all details, discernible by SEM: the exine sculpture is striate-reticulate with the striae mostly perpendicular to the polar axis and becoming parallel to the polar axis in the regions of poles and around the additional equatorial furrows. In TEM, the exine is 1.5–2.0 μm thick with a thick tectum, short columellae, foot layer and endexine; the infratectum, foot layer and endexine thicknesses are different throughout the pollen grain (for more information see Tekleva *et al.*, 2015).

According to Farabee (1993), *Pseudointegricorpus* belongs to a isopolar, strioreticulate long-colpate lateral-furrowed morphotype. This pollen genus is different from other genera of Triprojectate group by a unique feature – three lateral furrows transiting one into another in the equatorial region with endexineous thickenings that might be considered similar to an endocingulum. The three furrows might be also considered as one circular aperture. In modern plants, pollen grains with three lateral furrows are unknown. Some botanical affinities of *Pseudointegricorpus clarireticulatum* can be searched among pollen with an endocingulum of members of the Polygonaceae, Apiaceae, Asteraceae, Apocynaceae, Caprifoliaceae, Sapotaceae and Solanaceae. At compression, the triprojectate condition of the fossil pollen could have been preserved due to the endexinous thickenings serving as supporting elements around the apertures.

The example of *Pseudointegricorpus* shows that CLSM has good perspectives for studies of medium-sized pollen with a complicated exine structure and can help one to examine in detail all sides and structures (such as apertures, projections, and thickenings) of the pollen grain and to make measurements of some sculpture elements and exine layers (Table 1). The main advantage of CLSM is its ability to indicate the exact location of all visible and concealed (inner) pollen structures in the sporoderm; this helps one to correct the description of the taxon and to choose the necessary position of further ultrathin sectioning for a TEM study. The exine sculpture and some ultrastructural details can be distinguished rather clearly. Other elements (sporoderm ultrastructure) are indistinguishable or poorly seen in CLSM. Some difference in the exine thickness throughout the pollen grain can be the cause of the discrepancy between the measurements of the exine thickness in CLSM and TEM.

Pollen grains of *Wodehouseia spinata* (Figs. 4A–J; Tekleva *et al.*, 2012) are ellipsoidal, medium-sized, about 25 × 32 μm. LM shows that the pollen grains have an echinate surface and a thick columellate exine; pores are not always clearly seen (Figs. 1A, B). The pollen grains are compressed in course of fossilisation (Figs. 4C, H). CLSM measurements on virtual sections of a reconstructed pollen grain show that the total thickness in the central area of a compressed pollen grain (two exines and a obliterating gametophyte cavity between them) constitutes up to about 1.5–2.0 μm or up 5.0–5.5 μm (if to count echini). CLSM optical sections show a tectate columellate exine, which is about 4.2–4.7 μm thick in lateral areas of sections, with a thin tectum, high columellae, and no foot layer and/or endexine (Fig. 4G). Therefore, CLSM testifies that the exine thickness (without echini) of pollen grains of *W. spinata* pollen varies from 0.7 to 1.0 μm up to 4.0–5.0 μm depending on the location: the exine thickness is minimal in the central area of the pollen grain and maximal in a less compressed periphery. Pollen grains have four elongated pores (1.1 × 4.2 μm) perpendicular to the long axis of the pollen grain, with two pores on each side. Each pore is bordered with a large echinus about 2–3 μm in diameter at its base; the pollen grains have three types of echini: large echini around the pores and nearby, small echini on the peripheral region of the pollen and medium-sized echini in between. We can clearly see where the section passes in pollen grains reconstructed with help of CLSM (Fig. 4H). It is evident from CLSM images that the pollen is compressed in such a manner that pores on both sides are located opposite to each other and the pore is formed by a break in all exine layers (Figs. 4G, H). In SEM (like in LM), pores are not always clearly seen, but more details of the exine sculpture such as a perforated tectum (Fig. 4F) are distinguished in SEM in comparison to LM (Figs. 4A, B) or CLSM (Fig. 4E). In CLSM, virtual sections through a reconstructed compressed pollen grain differ from optical sections, compressed exine (measured in position of the pollen grain perpendicular to the long axis) is more than three times thinner than in the periphery and columellae are not distinguishable (Figs. 4G, H). In TEM, all exine layers are clearly seen and can be measured. It is evident that the exine thickness is unequal throughout the pollen grain, from 0.6 to 1.5 μm in a more compressed area of the pollen; a thin tectum, high and sometimes branched columellae and the inner layer (corresponding to the foot layer or endexine) of an uneven thickness are well-distinguished. TEM sections show (Fig. 4J) that the exine is thicker in less compressed peripheral areas reaching up to 4.0 μm, confirming our observations on optical sections obtained with LM and CLSM (Figs. 4A, G). There are cavities in lateral regions of the compressed pollen. TEM measures that the total thickness of the pollen in a compressed state (two exines and a compressed gametophyte cavity between them) is about 2–2.5 μm without echini. The echini are solid, and the pores are represented by a break in all exine layers; they are located opposite to each other.

Pollen grains of *Wodehouseia* belong to the so-called 'oculata' group (Chlonova, 1961) together with several other pollen genera of unknown botanical affinities which also have been found only in dispersed state so far. The unusual morphology, aperture condition and sporoderm ultrastructure of *Wodehouseia* do not find convincing analogues both among known fossil and modern taxa. Some parallels can be run with a number of modern taxa having pollen with four pores or short colpi such as Acanthaceae (*Adathoda*, *Beloperone* and *Justicia*), Anacardiaceae (*Pistacia*), Apocynaceae (*Nerium*), Balanophoraceae (*Langsdorffia*), Balsaminaceae (*Impatiens*), Betulaceae (*Alnus* and *Carpinus*), Bromeliaceae (*Aechmea*, *Hohenbergia*), Campanulaceae (*Adenophora*, *Asymeuma*, *Campanula* and *Phyteuma*), Connaraceae (*Jollydora*), Euphorbiaceae (*Picrodendron* and *Suregada*), Haloragaceae (*Myriophyllum*), Icacinaceae (*Alsodeiopsis*, *Desmostachys*, *Natsiatum* and *Theligonum*), Malpighiaceae (*Triaspis*), Malvaceae (*Hoheria*), Olacaceae (*Anacolosa*, *Cathedra*, *Harmandia* and *Ptychopetalum*), Polemoniaceae (*Collomia*), Rubiaceae (*Lasianthus*), Rutaceae (*Erythrochiton*) and Trigoniaceae (*Trigonia*), but details of the exine sculpture and especially

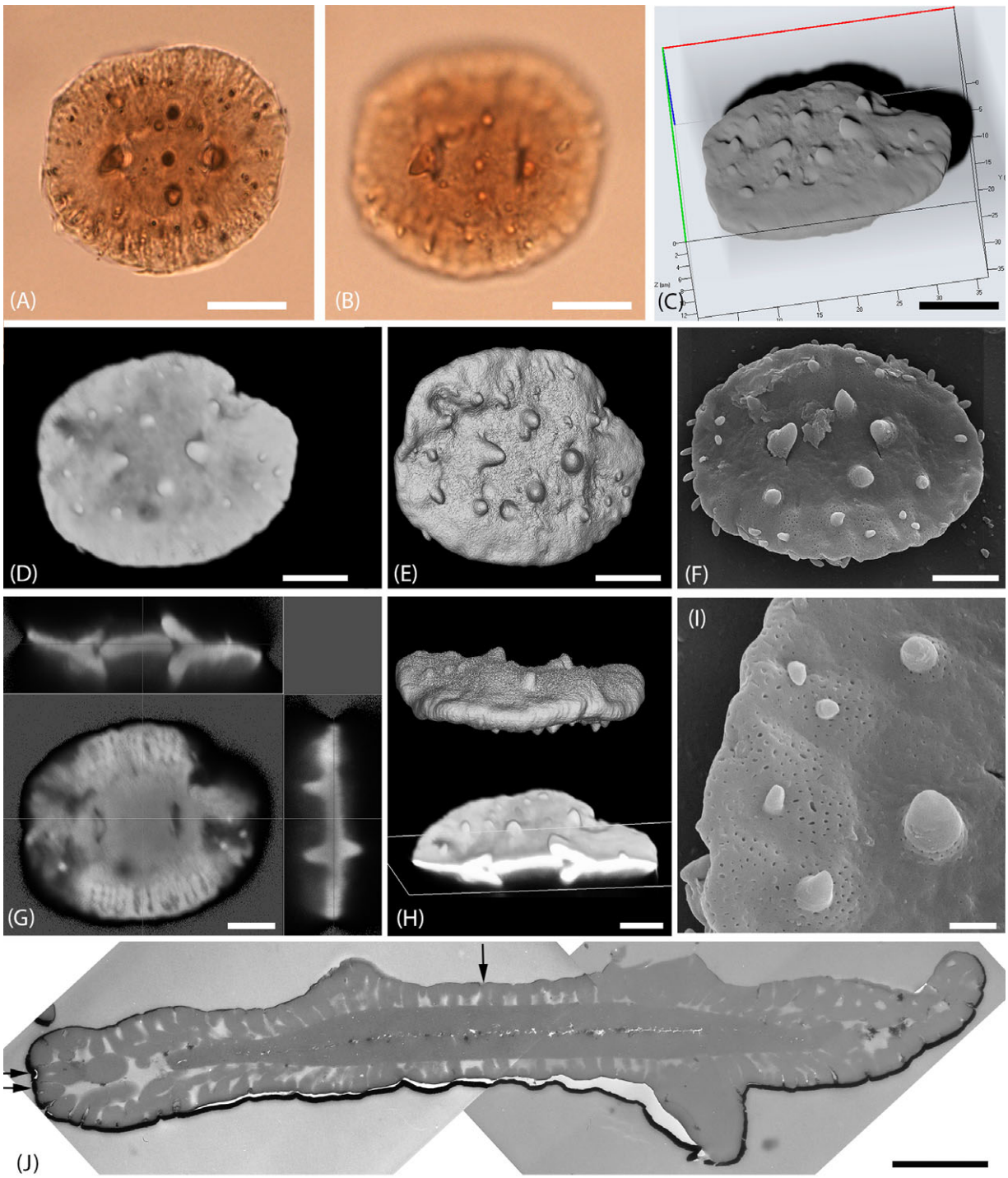

Fig. 4. Pollen of *Wodehouseia spinata*. (A, B) LM; (C–E, G, H) CLSM; (F, I) SEM; (J) TEM. (A, B) Pollen grain, different foci, two distinct pores and echinate pollen ornamentation are seen; (C) reconstructed pollen grain, shadow mode; (D) reconstructed pollen grain, transparent mode; (E) reconstructed pollen grain, surface mode; (F) an overview of the pollen, two pores and differently sized echini are seen; (G) optical sections ortho, lines of sectioning are shown, exact location of apertures is clearly seen; (H) an overview of compressed part of pollen grain, in surface mode (upper image) and a section through reconstructed pollen, transparent mode (lower image); (I) close up of the surface, differently sized echini and perforated tectum are seen; (J) section of a whole pollen grain, the exine is of uneven thickness with a thin tectum, columellate and sometimes branched infratectum, lateral cavities and solid echini; arrow points on the thinnest area of the exine and double arrow – on the thickest exine in the periphery. Scale bars: (A–F) 10 μm; (G, H) 5 μm; (I–J) 2 μm.

sporoderm ultrastructure clearly contradict their possible relationships (see also discussion in Leffingwell *et al.*, 1970). Some analogues with occasional similar ultrastructures in fossil pollen (e.g. *Cordaitina rotata* (Luber) Medvedeva in Zavialova *et al.*, 2004) appear even less possible, due to the clearly angiospermous characters of *Wodehouseia* pollen.

Summing up, for *Wodehouseia* CLSM helps us to reveal cavities in the ectexine which are unclear in LM, to distinguish echinate sculpture with differently sized echini and the pore morphology and structure in more detail, and to make measurements of exine layers. Such pollen characters as perforations, inner exine layer and small lateral cavities in *Wodehouseia* are indistinguishable or poorly seen in CLSM.

Pollen grains of fossil gymnosperms

Pollen grains from seeds of *Allicospermum angrenicum* Nosova were quite poorly preserved (Figs. 5A–N). Earlier, we also studied pollen grains of *Cycadopites*, found in pollen chambers of dispersed seeds of *Allicospermum* spp. from the same locality (Zavialova *et al.*, 2014a,b). The pollen grains are oval in outlines and medium-sized (approximately 30 × 43 μm). The pollen grains were preserved as a densely packed group (Figs. 5A, J); they were pressed to each other and on cuticle fragments and repeatedly folded; and we failed to detach individual pollen grains from the group. As a result, we were not sure by LM observations whether the pollen grains are monosulcate or trisulcate (Figs. 5A–D), also keeping in mind that TEM observations revealed certain similarities to some trisulcate pollen grains of the *Eucommiidites*-type (Zavialova *et al.*, 2016). Surprisingly, TEM observations did not solve the problem, because it was difficult to differentiate between repeatedly folded exines of individual pollen grains (Fig. 5M). We saw thinned apertural regions, but were unsure how many apertural regions occur per one exine. CLSM showed that the cuticle has approximately the same fluorescence maximum as the exine has (Fig. 5E) and the thickness of the cuticle was comparable to that of the exine. We could not have separated the exines from the cuticle by means of CLSM software. Although in this case of pollen grains glued to the cuticle we could not have detected the apertural type via rotation of a pollen grain, but we did it by means of longitudinal and transverse virtual sections through reconstructions of the pollen grains; this way we revealed that only one thinned area is present in the exine and, therefore, the pollen grains under study are monosulcate (Figs. 5H, I). Virtual sections show that the exine is thin, about 1.5 μm in thickness, and appears homogeneous (Figs. 5H, I). The surface sculpture was undetectable (Fig. 5F).

In sum, CLSM allowed us to show clearly that the sulcus is solitary (on the basis of virtual sections through reconstructed pollen grains). We were able to measure roughly the exine thickness in the apertural and nonapertural areas even in a mechanically damaged pollen grain. The measurements of the total exine thickness in apertural and nonapertural regions obtained by CLSM do not contradict to those obtained by TEM (Zavialova *et al.*, 2016). However, CLSM did not reveal the exine sublayers as well as their ultrastructure and relative thicknesses: the three-layered ectexine of a thick solid tectum, a thinner alveolate infratectum, a very thin foot layer and a homogeneous endexine were detected by TEM (Fig. 5M), but remained invisible via CLSM (Figs. 5H, I). SEM observations (Figs. 5J–L, N) showed that a fine and rather indistinct pattern is present on the pollen surface (Figs. 5L, N), though it was undetectable with CLSM (Fig. 5F). Our comparison showed that measurements of the general sizes of pollen grains based on CLSM is often by 1–2 μm higher (pollen grains appear longer and/or wider by 1–2 μm) than those based on LM. We suppose that the pollen grains are situated not completely flat and 3-D reconstructions reflect this difference.

Megaspores of fossil lycopsids

Dispersed megaspores identified as *Maexisporites rugulaeferus*, *M. grosstriletus* and *Trileites* sp. have been studied with CLSM; data obtained by other microscopes were used for comparison: *M. rugulaeferus* – LM, SEM and TEM; *M. grosstriletus* – SEM and *Trileites* sp. – LM. All megaspores are trilete with a thick ornamentated exine (Figs. 6–8; Karasev & Turnau, 2015). With LM we can describe the general morphology and outlines of megaspores and measure the sporoderm thickness; proximal scars are not always detectable, and the position of some observed elements was not completely understood, whether they were situated on the surface or within the sporoderm (Figs. 6A, B, 8A–D).

Megaspores of *Maexisporites rugulaeferus* are quite large and were first studied in transmitted light with an objective ×40 (Figs. 6A, B). It turned to be impossible to reconstruct the entire spore, because the sporoderm was too thick to let the ray pass. We reconstructed one hemisphere of the spore and visualised the surface (Fig. 6C). When we reconstructed a portion of the sporoderm with an objective ×100, some information about the sporoderm inner structure was obtained in virtual sections (Figs. 6D, F–I). The sporoderm is up to 15 μm thick, two-layered. The outer layer is up to 10 μm thick, dense, and appears to be composed of fine granules about 0.3 μm in diameter (Fig. 6D). The inner layer is lamellate, up to 5 μm thick; the lamellae are about 1 μm (Fig. 6D). When we broke the megaspores, we succeeded to scan portions of their sporoderms and revealed that their inner layer is a film that forms folds (Figs. 6E–I).

The megaspores turned to be too large and thick-walled objects for a CLSM study. Because we were forced to break the spore and observe its pieces, CLSM was a destructive method in this case. The surface pattern was reconstructed with CLSM too roughly by comparison to SEM images (compare Figs. 6C and 6J, K). As the comparison of semithin (Fig. 6L) and ultrathin sections (Fig. 6M) shows, CLSM allowed us to measure

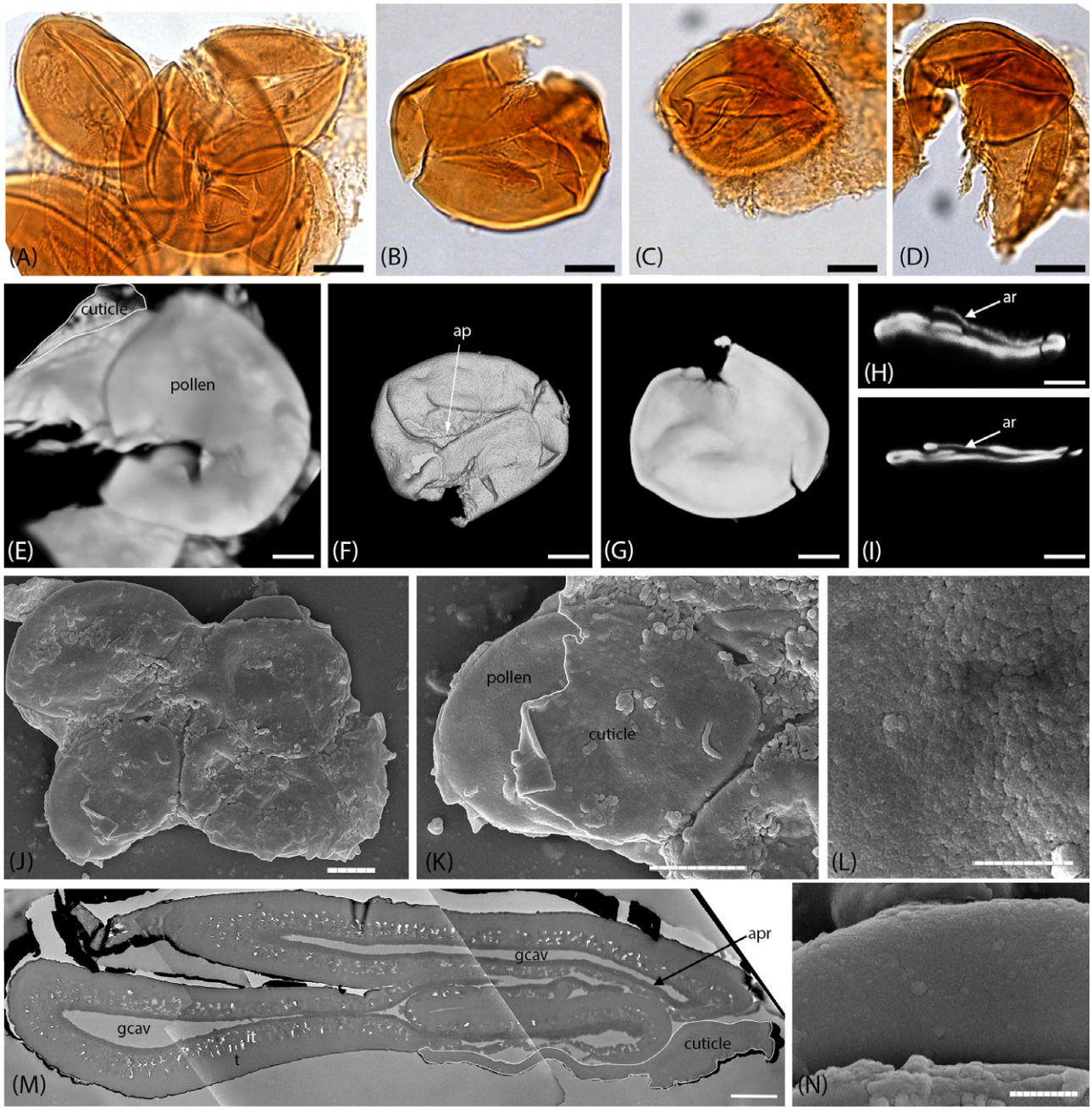

Fig. 5. Pollen grains from seeds of *Allicospermum angrenicum*, specimen BIN 813–79: (A–D) LM; (E–I) CLSM; (J–L, N) SEM; (M) TEM. (A) Group of compressed pollen grains on the cuticle; (B) a damaged detached pollen grain; (C) pollen grain on a folded cuticle; (D) damaged pollen grains on the cuticle; (E) reconstruction of two damaged pollen grains on the cuticle, which are shown in (D) transparent mode; (F) reconstruction of a pollen grain is shown in (B), distal face and aperture (ap) are shown, surface mode; (G) reconstruction of the same pollen grain that is shown in (F), proximal face is shown, transparent mode; (H, I) virtual sections through reconstructed pollen, a thinning in the apertural region (ar) is evident; (J) group of four pollen grains, covered with a cuticle; (K) blowing up of (J), a pollen grain partially covered with a cuticle; (L) blowing up of (K) showing the surface pattern of the pollen grain; (M) section through several pollen grains on the cuticle, tectum (t), infratectum (it), gametophyte cavity (gcav) and aperture region (ar) are visible; (N) magnified part of a pollen grain showing sculpture details. Scale bars: (A–K) 10 μm; (L, N) 2 μm; (M) 1 μm.

the entire thickness of the sporoderm quite correctly. CLSM also was able to reveal that the sporoderm is two-layered, and both of the layers are nonhomogeneous. However, fine granules that are reconstructed by CLSM as structural elements of the outer sporoderm layers (Figs. 6D, H, I) are in fact branching units, as is proved in semithin sections (Fig. 6L) under SEM (this way 3-D structure can be in part visible) and by tracing outlines of structural elements in a series of adjacent

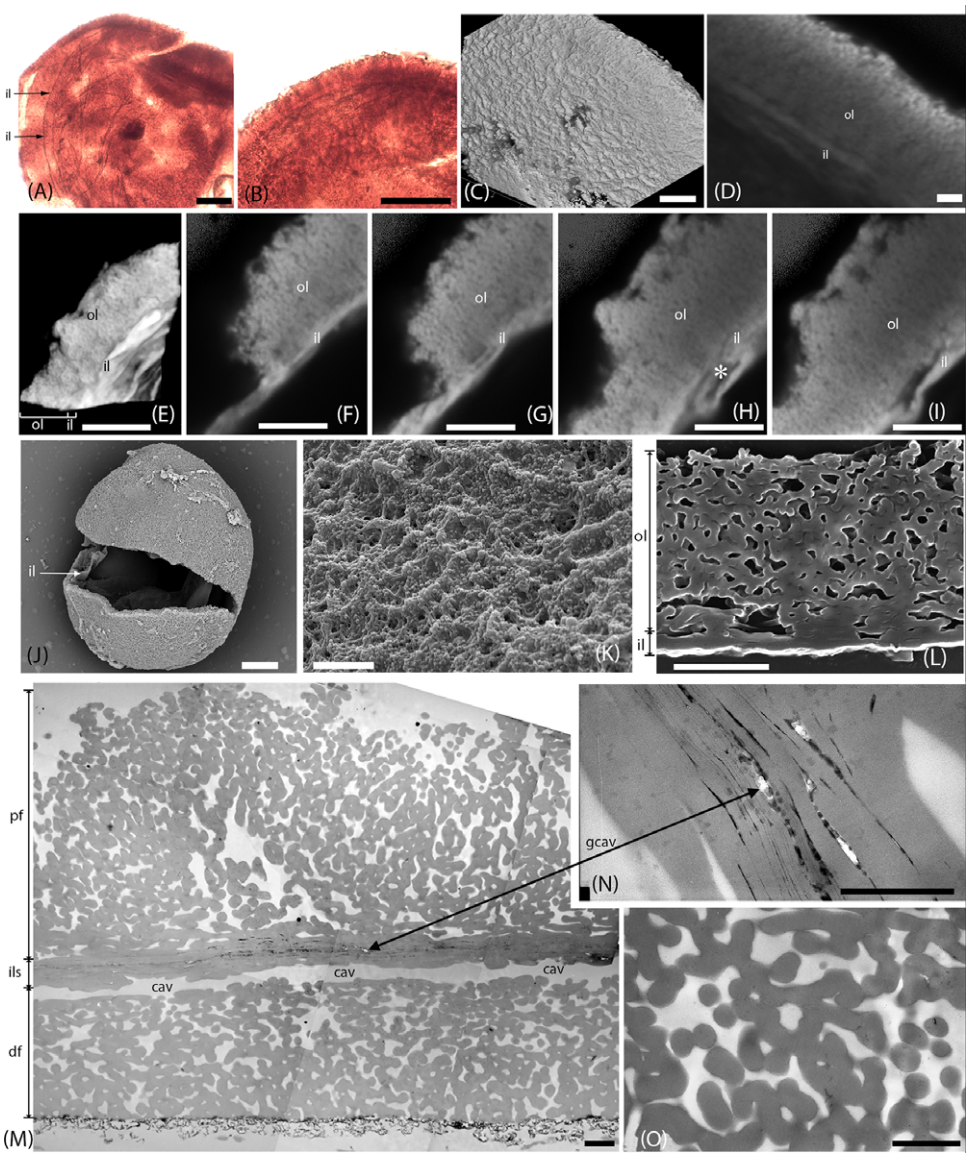

Fig. 6. Megaspores of *Maexisporites rugulaeferus*. (A, B) LM; (C–I) CLSM; (J–L) SEM; (M–O) TEM. (A) A folded inner layer (il) is visible through the outer layer; (B) focus on the sporoderm structure; (C) reconstructed part of sporoderm, surface pattern, transparent mode; (D) optical section through sporoderm, inner (il) and outer (ol) layers are distinguishable; (E) reconstructed part of sporoderm was rotated to demonstrate outer (ol) and inner (il) layers; (F–I) optical sections of reconstructed part of the sporoderm (E) at different depths of the sporoderm, the inner layer (il) of sporoderm forms fold (H) (asterisks) or is partly separated from the outer layer (ol) (H, I); (J) general view of a mechanically damaged spore, inner sporoderm layer (il) is visible inside the spore and is partly separated from the outer layer; (K) spore sculpture; (L) semithin sections through proximal sporoderm, note the horizontal direction of structural units in the inner part of the outer sporoderm layer and variously directed structural units closer to the sporoderm surface, the outer layer (ol) and inner layer (il) are distinct, and the internal surface of the latter can be observed; (M) sporoderm in the proximal scar area with outer layers of the proximal (pf) and distal (df) faces, proximal and distal inner layers (ils) are fused and gametophyte cavity (gcav) between them is obliterated, whereas a cavity (cav) in the distal sporoderm is evident; (N, O) enlargements of parts of (M); (N) lamellae of fused proximal and distal inner layers, gametophyte cavity is obliterated; (O) branching elements are cut at various angles, their cross sections imitate granules. Scale bars: (A, J) 50 μm; (B, C) 20 μm; (D, E, K, L) 5 μm; (F–I) 10 μm; (N) 0.5 μm; (M, O) 1 μm.

ultrathin sections (Fig. 6M). Circular elements, visible in ultrathin sections (e.g. Fig. 6O), are cross sections of cylindrical elements with variously directed branches. This type of the ultrastructure is common among fossil megaspores of a supposed lycopsid affinity. We should acknowledge that such sporoderms are quite often erroneously reported as granulate even on the basis of TEM, if the description of the ultrastructure is based on solitary ultrathin sections rather than on the

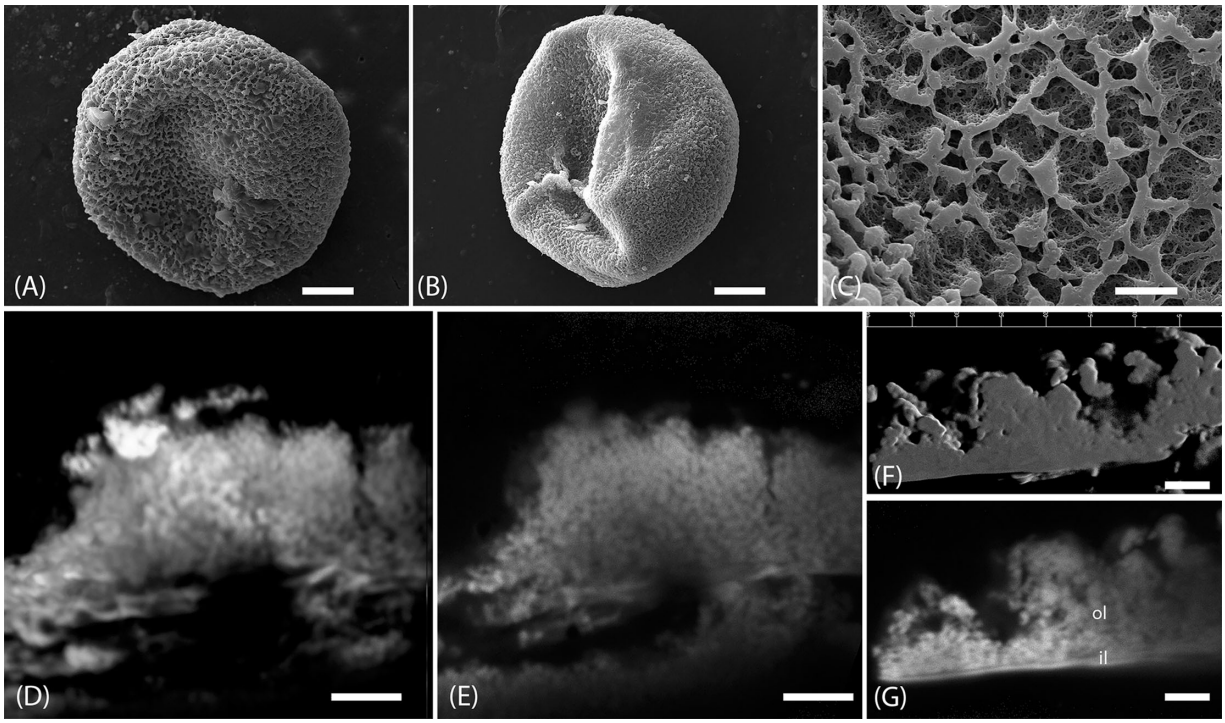

Fig. 7. Megaspore of *Maexisporites grosstriletus*. (A–C) SEM, (D–G) CLSM. (A, B) Spore general view in distal (A) and proximal (B) positions; (C) spore surface pattern; (D, E) optical sections through part of sporoderm at different depths; (F) reconstructed part of sporoderm, shadow mode; (G) the same reconstructed part of sporoderm, transparent mode, inner (il) and outer (ol) layers are distinguishable. Scale bars: (A, B) 50 μm; (C) 10 μm; (D–G) 5 μm.

analysis of a series of adjacent sections and on semithin sections. TEM confirms that the inner sporoderm layer is lamellate (Fig. 6N); however, the lamellae are much more numerous and much thinner than it was deduced in CLSM.

In sum, CLSM allowed us to get more information than LM about the general morphology, surface, and inner structure of the megaspore studied. The surface is better understood with SEM, whereas CLSM gives a simplified image of the surface. Both CLSM and LM revealed that the sporoderm is two-layered. CLSM, TEM and semithin sections in SEM showed that the upper layer is not homogeneous, but only a combination of TEM and SEM observations revealed the true nature of the structural elements. The lamellate nature of the inner layer is discernible only with TEM.

A megaspore of *Maexisporites grosstriletus* was about 300 μm in diameter (Figs. 7A, B). The megaspore was compressed in course of fossilisation. CLSM measures that in a compressed state its total thickness (proximal and distal sporoderms and gametophyte cavity between them) is about 70–80 μm. CLSM shows a two-layered sporoderm of 6–11 μm thick (Figs. 7D, E). The outer layer appears to consist of fine granules (Figs. 7D–G), which sometimes are arranged in lines. This layer varies in thickness considerably because of a smaller or greater amount of the structural elements (Fig. 7F). The inner layer is formed by a lamella about 0.5 μm thick (Figs. 6D, E, G).

Summing up, although we failed to scan this megaspore as an entity in good resolution, we were able to estimate the degree of its compression. To obtain any useful information about the inner structure with CLSM, we were forced to break the sporoderm and scanned portions of the sporoderm. This way we revealed that the sporoderm consists of two layers and estimated their thicknesses, but we not able to observe the surface pattern (Fig. 7C).

We succeeded to scan with CLSM a whole megaspore attributed to *Trileites* sp. (Figs. 8A–K). This spore is about 325 (314–336) μm in diameter and compressed up to 40–50 μm thick. The spore is trilete, with a distinctly elevated scar with long rays (Figs. 8A, B, E, F). The sporoderm is 7–9 μm thick (Fig. 8K), two-layered, with the inner layer about 1 μm thick (Fig. 8J). The inner layer lines the rays, elevating relatively high within the ray (Figs. 8I, J). A reticulum of branching variously directed elements is discernible in the outer layer (Fig. 8K). Spheroidal verrucae of 1–3 μm are visible on the surface. Groups of 'spherules' are located mainly in the equatorial region (Figs. 8C, G), optical sections show that each 'spherule' is connected with the outer sporoderm layer and apparently belongs to sculptural elements (Fig. 8K).

With CLSM, we observed a folded inner layer under the outer layer in the general view of the spore (Fig. 8F); the inner layer was present within the proximal scar; however, we did not find the inner layer in the equatorial region in virtual

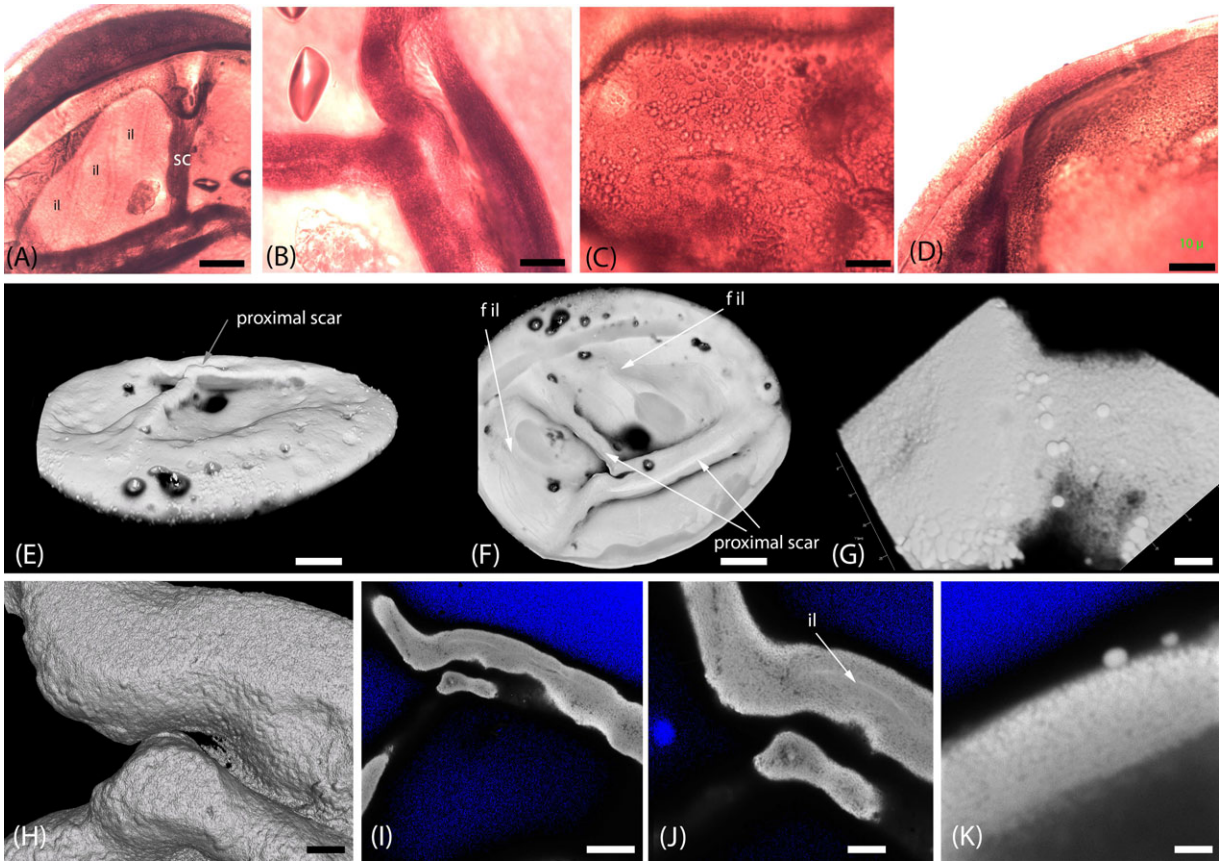

Fig. 8. Megaspore of *Trileites* sp. (A–D) LM, (E–K) CLSM. (A) The proximal scar is in part visible (sc) as well as folds of the inner layer (il), which are visible through the outer layer; (B, C) focus on trilete scar structure (B) and spore ornamentation (C); (D) focus on the sporoderm structure; (E) the reconstructed spore is tilted to show the degree of the spore compression, transparent mode; (F) inner part of reconstructed spore, folds of the inner layer (f il) are visible, transparent mode; (G) surface pattern of the spore in equatorial region, 'spherules' are detectable, transparent mode; (H) proximal scar, surface mode; (I, J) optical section through the proximal scar; (J) enlargement of Figure 8(I), two layers of the sporoderm are detectable; (K) optical section through the sporoderm in the equatorial region, only the upper layer of the sporoderm (with 'spherules') is present. Scale bars: (A) 40 μm; (E, F) 50 μm; (B–D, G, H, I) 10 μm; (J, K) 5 μm.

optical sections (Fig. 8K). These observations indicate that the inner layer occupies a smaller area than the outer layer and is definitely attached to the outer layer proximally, but is not attached distally and equatorially. Therefore, the megaspore is cavate.

Application of CLSM to palynological objects

The position of CLSM in the hierarchy of microscopes is predetermined by its resolution, which is higher than that of conventional LM and lower than EMs. CLSM also can be grouped with LM when the microscopes are considered in relation to small palynological objects, because both microscopes allow one to study such objects without destroying them. This quality is particularly pertinent for palaeontological objects. Although CLSM reconstructs the surface pattern too roughly (elements that are finer than 0.3 μm are indistinguishable), and the totally reliable information about the sporoderm inner structure is mostly limited to the number of sublayers, their (roughly estimated) thicknesses, and homogeneous/nonhomogeneous state, CLSM can provide information that is unreachable by other microscopical methods.

We have tested pros and cons of CLSM for studies of fossil and modern palynological objects; we used for this purpose pollen grains and spores of different morphologies, botanical affinities, and preservation. CLSM data published by other authors were also evaluated in addition to the original data.

Angiosperm pollen grains are extremely diverse. As test objects, we have chosen among pollen grains of modern angiosperms a pollen type with a rather common (columellate) sporoderm ultrastructure and a pollen type with a very unusual sporoderm ultrastructure. Some other pollen types were earlier studied with CLSM, such as the commonest 3-colpate and 3-colporate pollen types (Liu *et al.*, 2009; Castro *et al.*, 2010; Gavrilova, 2012, 2014a,b; Sivaguru *et al.*, 2012,

2016; Mander & Punyacena, 2014), monoporate poaceous pollen (Salih *et al.*, 1997; Sivaguru *et al.*, 2012, 2016; Mander & Punyacena, 2014), sulcate pollen (Castro *et al.*, 2010), porate pollen and pollen amassed in polyads (Gavrilova, 2014b), and the *Croton*-pollen type (Sivaguru *et al.*, 2012, 2016). Saccate and nonsaccate types were studied among pollen grains of modern gymnosperms (Castro *et al.*, 2010; Gavrilova, 2014b; Mander & Punyacena, 2014). In palynology, CLSM is still not commonly used for various reasons; different methods and approach were utilised. The application of optical microscopic techniques to different palynomorphs shows that their success depends on the taxon studied (Castro *et al.*, 2010; Gavrilova, 2012, 2014b; Sivaguru *et al.*, 2012, 2016; Mander & Punyacena, 2014); the potency of CLSM visualisation is contingent on feature sizes (Gavrilova, 2012, 2014; Sivaguru *et al.*, 2012, 2016). For example, genera and species with monoporate pollen from the family Poaceae (Salih *et al.*, 1997; Sivaguru *et al.*, 2012, 2016; Mander & Punyacena, 2014) and 3-colporate pollen from the genus *Quercus* (Mander & Punyacena, 2014) have not been identified using CLSM because their pollen surface features that are diagnostic are too fine; SEM is needed to differentiate among genera within the Poaceae and species within *Quercus*. On the other hand, reticulate and striate 3-colporate pollen of *Nolana* or *Euonymus* species (Gavrilova, 2012, 2014a) can be distinguished with CLSM; similarly to SEM, CLSM was able to reveal all features of the pollen surface. Gavrilova (2014b) pointed to the unique ability of CLSM to show the inner structure of pollen which helped to reveal the number, size and location of pori in polyads of *Acacia* and the saccus structure in saccate pollen grains of *Cedrus.* Pollen morphological studies do not provide a comparison between CLSM and TEM data; only our paper shows the possibilities of confocal microscopy for the examination of the exine ultrastructure (Table 1).

CLSM, and, in particular, its ability to generate 3-D reconstructions of objects, turned to be very suitable for studies of angiosperm pollen grains possessing endoapertures. Apertures in pollen grains of different members of angiosperms are described by different authors in many ways, as simple (e.g. colpate) and compound (most often colporate) and evolutionary advanced apertures. This is because the margins of endoapertures (ora) often are not clear and can be poorly distinguishable in transmitted light. Occasionally, ruptures inside colpi are described as ora – CLSM helps to ascertain whether this aperture is colpate, colporoidate or colporate (Gavrilova, 2012). CLSM is most useful among available microscopes to understand the aperture type, because it allows one to make 3-D reconstructions of pollen grains and to observe their wall from the inside. Therefore, we are able to observe and describe endoapertures, as was shown for modern pollen of species of *Euonymus* (Gavrilova, 2012), *Nolana* (Gavrilova, 2014a) and *Datura* (present study). Wortley *et al.* (2015) analysed the morphology of angiosperm pollen grains in relation to modern phylogenies (APG III) and concluded that the inner structure and outlines of apertures are important characters, but they are difficult to be used because of data deficiency and difficulties in obtaining them. Without CLSM application, the internal surface of the exine revealing the endoaperture can be described only with help of SEM, on accidentally broken exines.

When ultrathin sections are made for TEM histological studies, semithin sections are simultaneously made to observe them in transmitted light and find the exact location of the area that should be examined within the embedded specimen under TEM. This practice is rarely suitable for palynological objects. They are usually too small and/or irregularly distributed in the block (if many pollen grains or spores are embedded in the same block). CLSM 3-D reconstructions of palynological objects and their further handling with help of CLSM software reveal the position of structures on the surface and inside pollen grains and spores, which helps to orientate the blocks properly during preparation for ultramicrosectioning. This way we can understand with more certainty which structure is present on a given TEM image and at which angle it was sectioned. This option is important in studies of any palynological object below 100 μm. Large pollen grains such as those of the Malvaceae or the genus *Cucurbita* (Cucurbitaceae) can be properly orientated under a dissecting microscope.

CLSM is helpful in studies of pollen grains bearing various appendages and having complicated exine structure. Rotation of 3-D reconstructions allows one to examine all sides and structures (such as apertures, projections, thickenings, cavities etc.) of the pollen grain, and to make measurements of some sculpture elements and, for some objects, exine layers. The main advantage of CLSM for such objects is its capacity to detect the exact location of all visible and concealed (inner) pollen structures in the sporoderm; this helps to correct description of the taxon and to choose necessary directions of further ultrathin sectioning for a TEM study, as it has been shown for modern and fossil angiosperms, particularly for pollen grains with a complicated morphology and for deformed pollen grains (Tekleva *et al.*, 2015; Zavialova *et al.*, 2016).

In our study of fossil gymnosperm pollen grains that are preserved in clumps and stuck to cuticles, CLSM helped us (more reliably than other microscopes) to understand the number of apertures. Virtual sections through a 3-D reconstruction of a group of pollen grains were orientated in a way to cut transversely one of the pollen grains at different levels and this way we clearly showed that the sulcus is solitary.

Morbelly & Rowley (1996) studied exospores of two species of modern *Selaginella* using CLSM and compared the results with TEM data. Different interpretations of the wall structure of *Selaginella* megaspores existed; their study of CLSM optical sections led these authors to the conclusion about its reticulate structure. We have attempted to use CLSM for our study of fossil megaspores. Generally, they are not very suitable objects for a CLSM study because of their relatively

large sizes and thick walls. However, we were able to show the degree of compression of fossil megaspores as well as the presence of a cavity between the outer and inner sporoderm layers and the disposition of sculptural elements. Useful information about the inner structure was obtained by scanning pieces of sporoderms. CLSM helps us to describe the general spore morphology and to obtain data about the inner morphology as cavities, folds, ray location etc. and some information about the sporoderm structure. The capability of CLSM for studying the inner structure of megaspores is highly dependent on the thickness and/or density of the sporoderm.

Application of CLSM is suitable if EMs cannot be applied. Even if fossil objects (like fossil pollen or spores) are only partially preserved, CLSM can provide useful information about the studied objects. Palynological objects processed for LM are observable with help of CLSM, in constant or temporary slides that are routinely used by palynologists. For example, Shute *et al.* (1996) applied CLSM to a historical material, a Late Silurian sporangium with thousands dyads of an unclear affinity. Only a nondestructive method was in demand, because the sporangium was enclosed in a constant Canada–Balsam slide as early as in 1937. CLSM turned to be useful in determining the topology of an internal membrane, and it additionally showed that the common wall between members of dyads displays a lesser degree of autofluorescence than the outer wall, that testifies to differences in their chemical composition. Scott & Hemsley (1993) observed fossil megaspores in polished coal blocks. CLSM provided sharper images of megaspore walls in comparison with LM images and facilitated a more secure identification of the spores under observation. The only other way to obtain ultrastructural information was to macerate the spore from the coal and process it for EMs.

Knowing the limitations of CLSM, one can obtain reliable information with application of this microscope. The present study has shown that CLSM can be successfully applied to different palynological objects without their additional staining, such as to pollen grains of modern and fossil seed plants and megaspores of fossil lycopsids. Some other plant objects can be studied in a similar manner, for example, seeds of modern angiosperms (our unpublished data) and cuticle remnants of fossil gymnosperms (compressions, Gavrilova *et al.*, 2015).

Conclusions

CLSM is a useful tool in palynological, particularly in pollen morphological, studies. This is a relatively simple technique. Its application leads to more realistic object imagining and opens new prospects in morphological, taxonomical and palaeobotanical investigations. The main advantages come from observations of optical sections and three-dimensional reconstructions and lead to understanding of inner structure of palynological objects. CLSM optical sections help us to clarify some sporoderm features; this option is essential if the pollen or spore cannot be dissected or destructed and a more informative TEM study is impossible by any reason. CLSM three-dimensional reconstructions of palynological objects allow the scientist to evaluate all morphological peculiarities and irregularities of the form of modern and fossil pollen grains and spores, estimate the degree of compression of fossil objects, and make correct descriptions and interpretations. Virtual sections through reconstructed pollen grains allow one to see 'unseeable'. However, all this possibilities depend on the sizes of the object and its constituting elements.

Acknowledgements

We are thankful to Prof. Sun Ge (Key-Lab for Evolution of Past Life, MOEC, Jilin University, Changchun and College of Paleontology, Shenyang Normal University, Shenyang, China), Dr. V.S. Markevich and Dr. E.V. Bugdaeva (Institute of Biology and Soil Science, Far East Branch, Russian Academy of Sciences, Vladivostok, Russia) for providing *Pseudointegricorpus* and *Wodehouseia* pollen grains, Dr. Natalya Nosova (BIN) for pollen grains from seeds of *Allicospermum angrenicum*, Dr. Roman Rakitov (PIN) for the assistance with SEM, and the head of Laboratory of Electron Microscopy of Lomonosov Moscow State University (Moscow) Georgii Davidovich and Olga Kostina (BIN) for the assistance with TEM. The study was carried out within the framework of institutional research project no. 01201255609 of the Komarov Botanical Institute of the Russian Academy of Sciences for OG and was supported by the Russian Foundation for Basic Research, nos. 14-04-00044, 16-04-00946 for NZ 15-04-06386 for OG and 17-04-01094 for MT, funding from the subsidy allocated to Kazan Federal University for the state assignment #5.2192.2017/4.6 in the sphere of scientific activities for EK.

References

Al-Quran, S. (2004) Pollen morphology of Solanaceae in Jordan. *Pakis. J. Biol. Sci.* **7**(9), 1586–1593.

Banks, H., Feist-Burkhardt, S. & Klitgaard, B. (2006) The unique pollen morphology of *Duparquetia* (Leguminosae: Caesalpinioideae): developmental evidence of aperture orientation using confocal microscopy. *Ann. Bot.* **98**(1), 107–115.

Castro, A.J., Rejon, J.D., Fendri, M. *et al.* (2010) Taxonomical discrimination of pollen grains by using confocal laser scanning microscopy (CLSM) imaging of autofluorescence. *Microscopy: Science, Technology, Applications and Education* (ed. by A. Méndez-Vilas & J. Díaz). Microscopy Book Series, 2010, 4, pp. 607–613. Formatex Research Center, Badajoz.

Chentsov, Y.S., Polyakov, V.Y. & Vagin, V.I. (1973) Ultrastruktura mitotichestikh khromosom na total'nykh preparatakh endosperma [Ultrastructure of mitotic chromosomes on total samples of endosperm of tulip]. *Proc. Acad. Sci. SSSR* **209**, 710–712.

Chlonova, A.F. (1961) *Spore and Pollen of the Upper Half of the Upper Cretaceous in the Eastern Part of the Western Siberian Lowland.* Trudy Inst. Geol. Geofiz. Sibirsk. Otd. Akad. Nauk SSSR, vol. **7**.

Christensen, P.B. (1986) Pollen morphological studies in the Malvaceae. *Grana* **25**(2), 95–117.

Erdtman, O.G.E. (1952) *Pollen Morphology and Plant Taxonomy. Angiosperms*. Almqvist & Wiksell, Waltham, Stockholm.

Farabee, M.J. (1993) Morphology of Triprojectate fossil pollen: form and distribution in space and time. *Bot. Rev.* **59**(3), 211–249.

Gavrilova, O.A. (2012) Confocal laser scanning microscope (CLSM) for identification of pollen grains: new possibilities. *Jap. J. Palynol.* **58**(8), 69.

Gavrilova, O.A. (2014a) Morphology of pollen grains of the family Nolanaceae. *Botanicheskij zhurnal* **99**(1), 82–90 (in Russian).

Gavrilova, O.A. (2014b) Application of confocal laser scanning microscopy to study pollen wall morphology. *Botanicheskij zhurnal* **99**(10), 1139–1147 (in Russian).

Gavrilova, O.A. & Tikhonova, O.A. (2013) Diversity of pollen grains shapes and their distribution across some Grossulariaceae species and hybrids. *Trudy KarNC*. (3), 82–92 (in Russian).

Gavrilova, O.A., Tikhonova, O.A., Ivanova, A.N., Kostina, O.V. (2017) Sporoderm structure and systematics of the genus *Ribes* (Grossulariaceae). *Proceedings of Moscow conference on plant systematics and morphology* (ed. by D.D. Sokoloff), pp. 141–145. MAKS, Moscow (in Russian).

Gavrilova, O.A., Zavialova, N.E., Tekleva, M.V. *et al*. (2015) Morphological and anatomical studies of fossil higher plants remains with help of confocal microscopy. *Proceedings of XIII Moscow conference on plant phylogeny* (ed. by A.K. Timonin), pp. 89–93. MAKS, Moscow (in Russian).

Golovko, V.V., Koutsenogii, R.P. & Istomin, V.L. (2011). Confocal scanning microscopy used to determine the volume and density of the pollen grains of siberian plants. *Interexpo Geo-Siberia*. **4**, 259–263 (in Russian).

Harley, M.M. (1986) The nature of the endoaperture in the pollen of Sapotaceae. *Pollen and Spores: Form and Function* (ed. by S. Blackmore & I.K. Ferguson). Linnean Society Symposium Series, vol. **12**, pp. 417–419. Academic Press, London.

Hemsley, A.R. (1990). The ultrastructure of the exine of the megaspores in two Palaeozoic seed-like structures. *Rev. Palaeobot. Palynol.* **63**(1-2), 137–152.

Hesse, M., Weber, M., Halbritter, H., Ulrich, S., Zetter, R., Buchner, R. & Frosch-Radivo, A. (2009) *Pollen Terminology: An Illustrated Handbook*. Springer Vienna, Vienna.

Hochuli, P.A. & Feist-Burkhardt, S. (2004) A boreal early cradle of Angiosperms? Angiosperm-like pollen from the Middle Triassic of the Barents Sea (Norway). *J. Micropalaeontol.* **23**(2), 97–104.

Hochuli, P.A. & Feist-Burkhardt, S. (2013) Angiosperm-like pollen and Afropollis from the Middle Triassic (Anisian) of the Germanic Basin (Northern Switzerland). *Front. Plant Sci.* **4**, 1–14.

Karasev, E. & Turnau, E. (2015) Earliest Triassic (Induan) megaspores from Moscow Syneclise, Russia: taxonomy and stratigraphy. *Ann. Soc. Geol. Pol.* **85**(1), 271–284.

Leffingwell, H.A., Larson, D.A. & Valencia, M.J. (1970) A study of the fossil pollen *Wodehouseia spinata*. I. Ultrastructure and comparisons to selected modern taxa. II. Optical microscopic recognition of foot layers in differentially stained fossil pollen and their significance. *Bull. Can. Petrol. Geol.* **18**(2), 238–262.

Liu, D., Chen, Z., Xu, H., Liu, W. & Wang, L. (2009) Reconstruction of 3D digital image of weeping *Forsythia* pollen. *Computer and Computing Technologies in Agriculture II, Volume* **1** (ed. by D. Li & C. Zhao). IFIP Advances in Information and Communication Technology, pp. 329–334. Springer US, Boston, MA.

Liu, F., Zhu, H. & Ouyang, S. (2011) Taxonomy and biostratigraphy of Pennsylvanian to Late Permian megaspores from Shanxi, North China. *Rev. Palaeobot. Palynol.* **165**(3–4), 135–153.

Mander, L. & Punyacena, S.W. (2014) On the taxonomic resolution of pollen and spore records of Earth's vegetation. *Int. J. Plant Sci.* **175**(8), 931–945.

Markevich, V.S., Bugdaeva, E.V., Ashraf, A.R. & Ge, S.U. (2011) Boundary of Cretaceous and Paleogene continental deposits in Zeya-Bureya Basin, Amur (Heilongjiang) River region. *Global Geol.* **14**(3), 144–159.

Maxwell, M.H. (1978) Two rapid and simple methods used for the removal of resins from 1.0 μm thick epoxy sections. *J. Microsc.* **112**(2), 253–255.

Morbelli, M.A. (1995). Megaspore wall in Lycophyta-ultrastructure and function. *Rev. Palaeobot. Palynol.* **85**(1), 1–12.

Morbelli, M.A. & Rowley, J.R. (1996) Application of confocal microscopy to exospore ultrastructure in megaspores of *Selaginella convoluta* and *S. marginata*. *J. Plant Res.* **109**(1), 37–44.

Nilsson, S. (1986) The significance of pollen morphology in the Apocynaceae. *Pollen and Spores: Form and Function* (ed. by S. Blackmore & I.K. Ferguson). Linnean Society Symposium Series, vol. **12**, pp. 359–374. Academic Press, London.

Peng, G.F., Zhou, S.M., Zhang, S.Q., Zhao, D.P., Zhang, Y.L. & Lu, A.M. (1985) Pollen morphology of Chinese *Datura* and its taxonomic significance. *Acta Phytotaxonomica Sinica* **23**(1), 29–35.

Persson, V., Knapp, S. & Blackmore, S. (1999) Pollen morphology and the phylogenetic analysis of *Datura* L. and *Brugmansia* Pers. *Solanaceae IV: Advances in Biology and Utilization* (ed. by M. Nee, D.E. Symon, R.N. Lester & J.P. Jessop), pp. 171–187. Royal Botanic Gardens, Kew.

Perveen, A. & Qaiser, M. (2007) Pollen morphology of family Solanaceae from Pakistan. *Pakis.n J. Bot.* **39**(7), 2243–2256.

Peyrot, D., Barrón, E., Comas-Rengifo, M.J., Thouand, E. & Tafforeau, P. (2007) A confocal laser scanning and conventional wide field light microscopy study of *Classopollis* from the Toarcian-Aalenian of the Fuentelsaz section (Spain). *Grana* **46**(4), 217–226.

Punt, W., Hoen, P.P., Blackmore, S., Nilsson, S. & Le Thomas, A. (2007) Glossary of pollen and spore terminology. *Rev. Palaeobot. Palynol.* **143**(1–2), 1–81.

Salih, A., Jones, A.S., Bass, D. & Cox, G. (1997) Confocal imaging of exine as a tool for grass pollen analysis. *Grana* **36**(4), 215–224.

Sangwan, R.S. & Sangwan-Norreel, B.S. (1980) Biochemical and structural aspects of induction and development of pollen-embryos in Datura. *Bulletin de la Société Botanique de France. Actualités Botaniques* **127**(3-4), 109–122.

Schopf, J.W., Calça, C.P., Garcia, A.K., Kudryavtsev, A.B., Souza, P.A., Félix, C.M. & Fairchild, T.R. (2016) In situ confocal laser scanning microscopy and Raman spectroscopy of bisaccate pollen from the Irati Subgroup (Permian, Paraná Basin, Brazil): comparison with acid-macerated specimens. *Rev. Palaeobot. Palynol.* **233**, 169–175.

Scott, A.C. & Hemsley, A.R. (1991) A comparison of new microscopical techniques for the study of fossil spore wall ultrastructure. *Rev. Palaeobot. Palynol.* **67**(1–2), 133–139.

Scott, A.C. & Hemsley, A.R. (1993) Controls upon the ultrastructural preservation of sporinite. *Fuel* **72**(8), 1145–1149.

Shute, C.H., Hemsley, A.R. & Strother, P.K. (1996). Reassessment of dyads contained in a late Silurian rhyniophytoid sporangium. *Spec. Pap. Palaeontol.* **55**, 137–145.

Siljak-Yakovlev, S. (1986) Functional dynamics of the pollen exine and apertures in compositae of the dinaric alps. *Pollen and Spores: Form and Function* (ed. by S. Blackmore & I.K. Ferguson). Linnean Society Symposium Series, vol. **12**, pp. 413–415. Academic Press, London.

Sivaguru, M., Mander, L., Fried, G. & Punyasena, S.W. (2012) Capturing the surface texture and shape of pollen: a comparison of microscopy techniques. *PloS one* **7**(6), e39129.

Sivaguru, M., Urban, M.A., Fried, G., Wesseln, C.J., Mander, L. & Punyasena, S.W. (2016) Comparative performance of airyscan and structured illumination superresolution microscopy in the study of the surface texture and 3D shape of pollen. *Microsc. Res. Techn.* https://doi.org/10.1002/jemt.22732

Tekleva, M., Markevich, V., Bugdaeva, E., Sun, G. & Gavrilova, O. (2015) *Pseudointegricorpus clarireticulatum* (Samoilovitch) Takahashi: morphology and ultrastructure. *Hist. Biol.* **27**(3-4), 355–365.

Tekleva, M.V., Markevich, V.S., Bugdaeva, E.V. & Sun, G. (2012) Morphology and ultrastructure of *Wodehouseia* pollen. *Jap. J. Palynol.* **58**(8 special issue), 234.

Wang, C., Lentini, Z., Tabares, E. *et al*. (2011) Microsporogenesis and pollen formation in cassava. *Biol. Plant.* **55**(3), 469–478.

Wortley, A.H., Hong, W., Lu, L., De-zhu, L. & Blackmore, S. (2015) Evolution of angiosperm pollen. 1. Introduction. *Ann. Mo. Bot. Gard.* **100**(3), 177–226.

Zavialova, N.E., Gomankov, A.V., Yaroshenko, O.P. & Rovnina, l.V. (2004) Morphology and ultrastructure of some monosaccate pollen grains of *Cordaitina* Samoilovich 1953 from the Permian of Russia. *Acta. Palaeobot.* **44**(1), 3–35.

Zavialova, N.E., Gordenko, N.V., Nosova, N.V. & Polevova, S. (2014a) The fine morphology of pollen grains from the pollen chamber of a supposed ginkgoalean seed from the Middle Jurassic of Uzbekistan (Angren locality). *Plant. Syst. Evol.* **300**(9), 1995–2008.

Zavialova, N. & Karasev, E. (2017) The use of the scanning electron microscope (SEM) to reconstruct the ultrastructure of sporoderm. *Palynology* **41**(1), 89–100.

Zavialova, N., Nosova, N. & Gavrilova, O. (2016) Pollen grains associated with gymnospermous mesofossils from the Jurassic of Uzbekistan. *Rev. Palaeobot. Palynol.* **233**, 125–145.

Zavialova, N., Polevova, S., Tekleva, M. & Bogdanov, A. (2017) Prospects of methods for studies of fossil sporoderm. *Bull. Mosc. Soc. Natural. (Biol.)* (in Russian) **122**, in press.

Zavialova, N.E., Tekleva, M.V., Gavrilova, O.A., Nosova, N.V., Gordenko, N.V., Markevich, V.S. & Bugdaeva, E.V. (2014b) Prospects of confocal microscopy for morphological studies of fossil pollen and spores by comparison to electron microscopy. *Paleostrat-2014. Annual meeting of paleontological section of Moscow Society of Naturalists and Moscow Branch of Russian Paleontological Society. Abstracts. (Moscow, January 27–29, 2014)* (ed. by A.S. Alekseev), pp. 31–32. PIN RAS, Moscow (in Russian).

Zhuo, E., Tang, L. & Zhang, H. (2006) Application of laser scanning confocal microscope in fossil spore-pollen observation. *Acta Palaeontologica Sinica* **45**(3), 430–436.